Key Points:

- The brightening/dimming record of surface solar radiation over the U.S. has been updated through 2019
- Brightening over the U.S. that began in the 1980s seems to have ended in 2012
- Surface brightening and dimming trends in the U.S. since the 1990s have been attributed primarily to changes in cloud cover

Correspondence to:

J. Augustine,
john.a.augustine@noaa.gov

Variability of Surface Radiation Budget Components Over the U.S. From 1996 to 2019—Has Brightening Ceased?

John A. Augustine[1] and Gary B. Hodges[1,2]

[1]NOAA Global Monitoring Laboratory, Boulder, CO, USA, [2]Cooperative Institute for Research in the Environmental Sciences, University of Colorado, Boulder, CO, USA

Abstract The record of downwelling solar irradiance and other surface radiation budget components for the U.S. has been extended through 2019 using SURFRAD Network data. Brightening of surface solar irradiance of $+7.36$ Wm^{-2}/decade occurred from 1996 through 2012. In 2013, surface solar radiation sharply decreased to the long-term mean (representing 1996–2019) and remained near that level through 2017. Successive decreases in 2018 and 2019 yielded a dimming trend of -3.90 Wm^{-2}/decade after 2012, but with a high uncertainty owing to the observed variability and brief period covered. Individually, all stations but Penn State showed brightening trends consistent with the network average, and surface solar irradiance decreased at all stations after 2012. Total surface net radiation showed similar tendencies but the reversal from increasing to decreasing was more gradual because of the response of surface net longwave to the changing solar input. Aerosol optical depth decreased continuously throughout the tenure of the network but accounted for only 3% of the variability of surface solar irradiance, while cloud fraction explained 62%. The mean cloud fraction was 2.4% greater during the dimming period than the brightening period but showed no trends due to high interannual variability. However, annual anomalies of direct-normal solar radiation, which relate to sun duration and clouds, generally increased to 2012 and then decreased thereafter. Collectively, these results indicate that changing cloud cover was the primary source of brightening and dimming over the U.S. from 1996 to 2019.

Plain Language Summary Since the 1980s, it has been known that solar radiation at the surface of the Earth goes through increases (brightening) for two-to-three decades followed by decreases (dimming) over similar periods. These cyclic patterns are not caused by variations in the sun's emission but rather by changes in cloud cover and dust in the atmosphere. Brightening and dimming occur all over the globe. Dimming was documented in the U.S. from the 1950s to about the mid-1980s. In the mid-to-late 1980s, solar radiation at the surface reversed course and increased for more than 20 years. Here, we show that this most recent brightening period in the U.S. ended in 2012. Surface solar radiation decreased over the U.S. after 2013, signaling the possible beginning of a new dimming period. We determined that systematic changes in cloud cover were mostly responsible for these trends and that atmospheric dust played only a minor role. Knowledge of dimming and brightening is useful for research in weather, climate, agriculture, renewable energy, and any other process that responds to systematic changes of solar energy at the surface.

1. Introduction

Downwelling solar radiation at the surface (SW↓) goes through decadal-scale variations that are global in nature (Dutton et al., 2006; Gilgen et al., 1998; Hatzianastassiou et al., 2005, 2020; Herman et al., 2013; Liepert, 2002; Liepert et al., 1994; Ohmura & Lang, 1989; Stanhill, 2005; Stanhill & Moreshet, 1992; Wang, 2014; Wild, 2012; Wild et al., 2005, 2009; and others). A review by Wild (2012) reports dimming in the U.S. of -6 Wm^{-2}/decade from 1957 to the mid-1980s and brightening of $+6$ Wm^{-2}/decade from the mid-to-late 1980s well into the first decade of the 2000s. Augustine and Dutton (2013) independently show brightening over the U.S. of $+6.6$ Wm^{-2}/decade for their period of study of 1996 to 2011. Ohmura (2009) reports SW↓ trends in Europe of $+10$ Wm^{-2}/decade from the late 1930s to the 1950s, -13 Wm^{-2}/decade from the 1950s to the 1980s, and $+10$ Wm^{-2}/decade from the 1990s to 2005. The most recent updates for Europe (Sanchez-Lorenzo et al., 2015; Wild, 2016; Wild et al., 2021) indicate that brightening may have stopped there after 2010,

although the short time analyzed beyond 2010 is insufficient to establish an onset of an actual shift to dimming. Ohmura (2009) reports dimming of −6.3 Wm^{-2}/decade in Japan from 1960 to 1991 and then brightening of +6.2 Wm^{-2}/decade to 2008. Ohmura (2009) also shows continual dimming in India from the 1960s into the first decade of the 2000s, which is likely due to increased aerosols from industrialization and biomass burning (Thomas et al., 2019; Wild et al., 2009). Brightening on the Korean Peninsula from the 1990s to the early 2000s is documented by Wild et al. (2009). He et al. (2018) show dimming in China of −2.7 Wm^{-2}/decade from 1959 to 1989, then brightening of +8.6 Wm^{-2}/decade to 1995, followed by dimming of −1.0 Wm^{-2}/decade to 2010. Brightening from the 1990s to the early 2000s has also been reported for remote stations, including Antarctica (Dutton et al., 2006). According to Wild et al. (2009) brightening in Europe, the U.S., and Korea continued after 2000, but began to wane over other areas, stabilizing in Japan and Antarctica, while reverting to dimming in China and Central America. Wild (2012) concludes that these tendencies indicate the first decade of the 2000s may represent a transition from brightening to a more stable regime, or possibly the onset of dimming globally.

Documented magnitudes of brightening are significant and much larger than the projected increase in downwelling longwave radiation (LW↓) expected at the surface from the doubling of CO_2 since preindustrial times (∼4 Wm^{-2}), or the 11-year cyclical variability of solar output measured at the top of the atmosphere (∼1–2 Wm^{-2}; Ohmura, 2009; Willson & Mordvinov, 2003). Because brightening and dimming cycles are a primary source of energy variability at the earth's surface they have wide reaching implications for weather, solar energy production, agriculture, the hydrologic cycle, and any other system driven by available energy at the surface. For example, Müller et al. (2014) show that brightening from the 1990s to 2010 enhanced tracked-plane-solar-panel energy production by 8.5%/decade, and Tollenaar et al. (2017) attribute a 27% boost of the U.S. Corn Belt yield trend to brightening between 1984 and 2013.

Variability of solar irradiance at the surface may be caused by the direct, indirect, or semi-direct effect of aerosols. The latter is effective in more polluted regions where absorption/heating by aerosols may suppress cloud formation. Of course, a variety of regional climate processes can also change cloud distributions, including fluctuations in storminess, El Niño cycles, and decadal variations in ocean conditions such as the Pacific and Atlantic multidecadal oscillations of sea surface temperatures (e.g., Alexander et al., 2014; Chylek et al., 2014; Enfield et al., 2001; McCabe et al., 2004; Nigam et al., 2011; Sutton & Dong, 2012; Ting & Wang, 1997; Wang et al., 2014; and others). Concerning changes in cloudiness itself, Hatzianastassiou et al. (2005) argue that changes in planetary Hadley and Walker circulation patterns caused by changes in solar heating at the surface can also systematically alter cloud patterns. They show a decrease in low-level clouds in tropical and subtropical regions was responsible for ∼70% of the brightening from the 1990s to the early 2000s. Augustine and Dutton (2013) and Long et al. (2009) find a systematic reduction in cloud cover primarily responsible for brightening over the U.S. during that same period. Ohmura and Lang (1989) attribute European dimming from the late 1950s to the late 1980s to varying cloud conditions. Wild (2009, 2012) generally conclude dimming in Europe from 1952 to the 1980s coincided with increasing aerosols, but brightening during the 1990s corresponded to decreasing aerosols and their attendant effect on cloud cover, or other meteorological effects. Stanhill and Moreshet (1992) attribute dimming in Europe from 1958 to 1985 to aerosols at four stations and clouds at three.

This update of surface radiation tendencies in the U.S. through 2019 shows that the brightening that began in the mid-to-late 1980s ended in 2012. In 2013 surface solar irradiance decreased sharply to near the long-term mean (representing 1996–2019), and showed only slight variability for the next 5 years, followed by consecutive decreases in 2018 and 2019. This pattern suggests that the U.S. may have entered the initial phase of a new dimming period. The discussion that follows considers the roles of aerosols and clouds in this process.

2. The U.S. SURFRAD Network

The SURFRAD surface radiation budget network (Augustine et al., 2000, 2005) has seven stations that together reasonably represent the surface radiation climatology of the U.S (Figure 1). A cross-correlation of SW↓ annual averages with satellite estimates of surface solar irradiance from the International Satellite Cloud Climatology Project (ISCCP) (Dutton et al., 2006) applied to SURFRAD data (Augustine
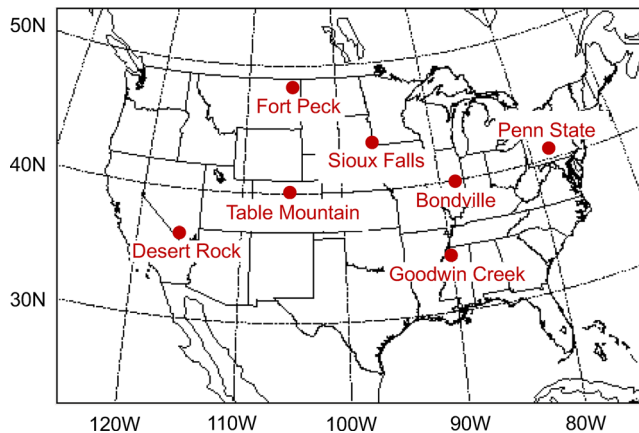
Figure 1. The U.S. SURFRAD network.

et al., 2006) shows that a network annual average of SW↓ represents at least 70% of the contiguous U.S. land area. This finding is consistent with Sanchez-Lorenzo et al. (2015) who demonstrate that SW↓ trends from five stations spaced somewhat evenly across Europe show the same trends as 56 stations.

2.1. Instrumentation and Derived Products

Operational practices at SURFRAD stations follow recommendations of the World Meteorological Organization's (WMO) Baseline Surface Radiation Network (BSRN) (McArthur, 2005; Ohmura et al., 1998). Thermopile-based pyranometers are used for broadband shortwave measurements because they are sensitive to nearly the full range of the solar spectrum reaching the surface. All radiometers used for basic surface radiation budget (SRB) measurements are classified as "WMO class 1" except the Eppley model 8–48 pyranometer, which is used for the diffuse solar measurement. Although designated as "class 2" by the WMO, the model 8–48 has no appreciable thermal offset (Bush et al., 2000; Gueymard & Myers, 2008), and because it is shaded for the diffuse measurement its substandard angular dependency (cosine error) is not relevant. While total horizontal irradiance is collected by an unshaded single-black-detector pyranometer, it is considered secondary to the combination of the direct-normal and diffuse solar measurements. The latter, also known as the "component sum," is preferable because direct-normal and diffuse measurements lack the thermal offset and cosine errors that plague total horizontal irradiance measurements made with single-black-detector pyranometers (Bush et al., 2000; Gueymard & Myers, 2008; Ohmura et al., 1998). The cosine error of a single-black-detector pyranometer is particularly worrisome because the calibration value used is customarily set at 45° solar zenith angle (SZA) and then applied to measurements at all times of day. For obscured conditions, that is, no direct beam, there is no cosine error and the 45° calibration value is appropriate for the isotropic radiation of the diffuse sky. However, when the direct beam impinges on the detector the calibration of the pyranometer changes appreciably with solar position. Myers et al. (2002) demonstrate that a measurement from a single-black-detector thermopile-based pyranometer with the 45° SZA calibration applied can be in error by as much as 40 Wm^{-2} (~4%) near solar noon when the direct beam is present. In 2016, the Eppley Normal Incidence Pyrheliometer was replaced by the Kipp and Zonen CHP1 pyrheliometer at SURFRAD sites. According to Michalsky et al. (2011) the CHP1 is the most accurate pyrheliometer of all tested makes and models. The Eppley Precision Infrared Radiometer (PIR) is used for downwelling and upwelling broadband longwave measurements (~4,000–50,000 nm). A more detailed discussion of SURFRAD instrumentation can be found in Augustine et al. (2000, 2005).

Computed quantities used in this analysis are cloud fraction and aerosol optical depth (AOD). Cloud fractions are derived from the RadFlux analysis of Long and Ackerman (2000). The RadFlux cloud fraction algorithm was formulated by comparing diffuse solar measurements to measured cloud fractions from collocated Total Sky Imagers (Long et al., 2006). Accuracy of the computed cloud fraction is ±10%. AOD is derived from narrow band spectral measurements made by Multi-Filter Rotating Shadowband Radiometers (MFRSRs) (Harrison et al., 1994) using the method described in Augustine et al. (2003).

2.2. Calibrations and Quality Assurance

SURFRAD network operations incorporate robust quality assurance practices (Augustine et al., 2000). All broadband radiometers are calibrated prior to deployment using equipment traceable to world standards. Pyranometers and pyrheliometers are calibrated at the WMO Region four Solar Calibration Center at NOAA in Boulder, Colorado, USA. Their absolute cavity radiometer, which is the basis of all solar radiometer calibrations, is referenced to the World Radiometric Reference (WRR) (Fröhlich, 1991) every five years at the WMO International Pyrheliometer Comparison (IPC) at the Physikalisch Meteorologisches Observatorium Davos/World Radiation Center (PMOD/WRC) in Davos, Switzerland. It is also compared to a secondary standard from PMOD/WRC each interim year at the National Renewable Energy Laboratory Pyrheliometer Comparison in Golden, Colorado, USA. Uncertainties of calibrations range from 2% to 5% for pyranometers

and 1%–2% for pyrheliometers (Michalsky et al., 2011). Pyrgeometer calibrations are traceable to the World Infrared Standard Group (WISG) at PMOD/WRC, which is made up of two Eppley PIRs and two Kipp and Zonen CG4 pyrgeometers. Calibrations of the WISG standards are traceable to the IPASRC-I experiment (Philipona et al., 2001) and the blackbody calibration device at PMOD. For SURFRAD longwave calibrations three standard pyrgeometers are sent to PMOD/WRC biennially to be referenced to the WISG. The mean calibration of these three standards is transferred to field pyrgeometers via a side-by-side comparison before each deployment. This transfer results in pyrgeometer calibration uncertainties of approximately 5%.

All radiometers except MFRSRs are exchanged annually. This practice, and referencing instruments to accepted world standards before deployment, ensures accurate measurements and mitigates the effect of calibration drift on computed trends. The MFRSRs are continuously calibrated *in situ* for AOD analysis using the Langley method (Shaw, 1983). SURFRAD data are objectively verified and visually scrutinized on a daily basis before being released. These long-established practices of frequent high-quality world-reference-traceable calibrations and daily data quality control ensures that SURFRAD radiation data are continuous, accurate, and precise.

3. Data Analysis

One-minute averages of 1 Hz samples have been recorded at SURFRAD stations since January 1, 2009, and prior to that 3-minute averages of 1 Hz samples were collected. For the analysis presented, granular data were compiled into monthly averages and annual averages were computed from the monthly means. Because longwave contributes to the surface radiation budget over all hours, averages presented, including those of solar variables, include data from all 24 h of the day. Long-term means of each variable were computed for the period from each station's first full year through 2019. As in Augustine and Dutton (2013) and Long et al. (2009), annual averages were not analyzed directly because the stations represent differences in climate such that solar measurements at sunnier locations would receive greater weight in the network average. Instead, for all variables, annual anomalies from each station's long-term mean were analyzed. Station annual anomalies were averaged to form the network-wide results. For the seasonal analysis presented this process was repeated but using only the months within each season. The use of annual or seasonal averages for trend analysis reduces random error and expands the spatial influence of each station (Sanchez-Lorenzo et al., 2015; Schwarz et al., 2017).

At least 70% of accepted data (i.e., passed quality-control) for a particular station-month was required for an acceptable monthly average. New data analyzed for this study (2012 to 2019) were rather complete and the 70% threshold came into play only once for the May 2018 average of surface reflected solar (SW↑) at Table Mountain. When a monthly average was not acceptable, empirical gap-filling methods were used in lieu of climatological averages. For example, to get a proxy reflected solar value for May 2018 at Table Mountain the mean monthly albedo of its boundary months were averaged and multiplied by the monthly mean SW↓ for May 2018 to produce a substitute SW↑ value [see Section 3.2 of Augustine and Dutton (2013) for more information on gap-filling methods]. The component sum (direct + diffuse) was used for SW↓. For times when direct or diffuse solar measurements were not available, the secondary measurement from a co-located single-black-detector pyranometer was substituted. Leveraging this versatility, SW↓ had just under 100% coverage from 2012 to 2019. Increased error from the use of the stand-alone pyranometer for SW↓ was not a concern because the component sum was available over 99% of the time at all stations. Only four other station-months of SRB-critical quantities had less than 99% coverage, and the least of those was 98%.

4. Results

4.1. Trends in U.S. Surface Radiation

Time series of surface SW↓ annual anomalies from 1996 to 2019 are shown in Figure 2. Periods from 1996 to 2012 and 2013 to 2019 are treated separately because of a change in character of surface radiation after 2012. The network average time series is shown with those of individual stations overlaid to illustrate the variability contained in the average. Brightening dominated from the start of the network through 2012 with SW↓ increasing at a rate of $+7.36 \pm 1.47 \, \mathrm{Wm}^{-2}$/decade. That trend is statistically significant according to the non-parametric Mann-Kendall (MK) test (Kendall, 1975; Mann, 1945) and has a small uncertainty. Despite
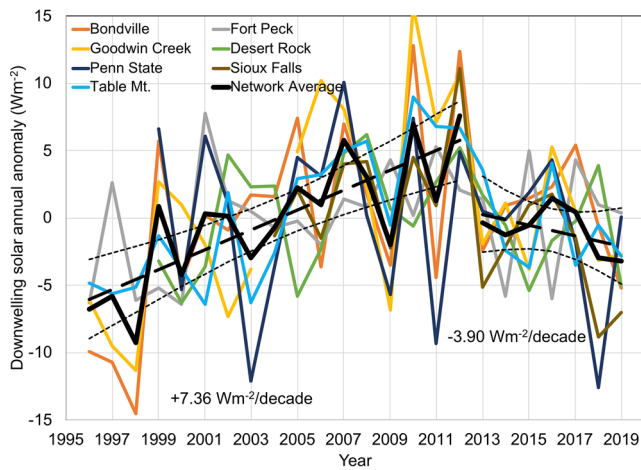
Figure 2. Time series of SW↓ annual anomalies for the SURFRAD Network. The horizontal zero line represents the long-term average over the length of each time series. Network average annual anomalies are denoted by the thick black curve, and color-coded curves are annual anomalies of individual stations. Thick black dashed lines are linear least-squares fits to the network average time series computed separately for 1996–2012 and 2013–2019. Thin black curved dashed lines are 95% confidence intervals of the linear fits.

interannual variability, SW↓ generally increased at all stations but Penn State over that period. In 2013, the character of SW↓ changed dramatically at all stations. The network average dropped to near the long-term mean and varied by ∼±1 Wm^{-2} for the next four years. In 2018, the network average declined, although Penn State and Sioux Falls contributed most to that down-turn, and then decreased again in 2019. A decreasing trend of -3.90 ± 3.1 Wm^{-2}/decade was computed for 2013 to 2019, but there were too few points for MK analysis to reliably determine statistical significance. Also, the uncertainty of the trend is nearly as large as the trend itself and thus can only indicate a declining tendency between -0.8 and -7.0 Wm^{-2}/decade took place during this latter period. However, that each station's SW↓ time series changed similarly after 2012 confirms a robust change in the character of surface solar radiation took place and hints that the U.S. may have entered a new period of dimming. This result supports the assertion of Wild ([2012]) that the early 2000s could possibly be a transition period from brightening to dimming.

Tests were conducted to determine if some stations contributed disproportionately to the network average. First, each station was dropped sequentially from the sample and the resulting 6-station annual averages were compared to the full network annual average by means of linear least squares. Measures of compatibility were quantified by the R^2 values and the trends within the brightening period. The results in Table 1 shows that brightening trends of the seven permutations all had low uncertainty and that no one station dominated the national average. To assess whether brightening and dimming trends were uniform throughout the network, trends at the individual sites were examined. Brightening trends were greatest at Bondville (9.5 ± 3.1 Wm^{-2}/decade), Goodwin Creek (10.9 ± 2.9 Wm^{-2}/decade), Table Mt. (8.6 ± 1.5 Wm^{-2}/decade), and Sioux Falls (8.6 ± 4.7 Wm^{-2}/decade), and moderate at Fort Peck (4.3 ± 1.8 Wm^{-2}/decade) and Desert Rock (5.2 ± 2.5 Wm^{-2}/decade). Penn State showed very high interannual variability and no trend through 2012. Considering the margin of error associated with each trend, all stations but Penn State show increasing SW↓ in the brightening period. Furthermore, all sites, including Penn State, reveal a dramatic drop in surface solar radiation after 2012, as shown by individual station time series in Figure 2. These results suggest that brightening occurred over much of the U.S. from 1996 to 2012 with the possible exception of the Northeast, and that the dimming that followed took place over the entire network.

Figure 3 shows the long-term variation of total surface net radiation ($Q^* = SW\downarrow - SW\uparrow + LW\downarrow - LW\uparrow$) over the network. The positive trend of the network mean Q^* in the brightening period (8.2 ± 1.0 Wm^{-2}/decade) is statistically significant according to MK analysis. Also, the decline of Q^* after 2012 of -4.07 ± 2.0 Wm^{-2}/decade is less uncertain than the trend of SW↓ during that period. Similarity of the Q^* and SW↓ time series is a consequence of the dominance of downwelling solar on total surface net radiation. As with SW↓ in Figure 2, each station's time series of Q^*, except Penn State, evolves in a similar manner indicating that a robust change in Q^* has also taken place over most of the network. One difference is that the reversal from increasing to decreasing Q^* is not as abrupt as that of SW↓. Surface net radiation increases at a slightly larger rate than SW↓ during the first part of the brightening period but the upward trend slows after 2005. This

Table 1
Linear Regression R^2 Values and Trends of Annual Network Average Surface Solar Irradiance (1996–2012) for Permutations With One Station Removed versus the Full Network

Station not included	Without Bondville	Without fort peck	Without Goodwin Creek	Without Table Mountain	Without desert Rock	Without Penn state	Without Sioux Falls
6-station R^2	0.9704	0.9723	0.9588	0.9782	0.9784	0.9616	0.9930
6-station brightening trend (Wm^{-2}/decade)	6.65 (±1.26)	8.20 (±1.80)	6.64 (±1.44)	7.30 (±1.66)	7.42 (±1.68)	7.95 (±1.23)	7.35 (±1.48)

The station named at the head of each column is the station removed for that permutation.
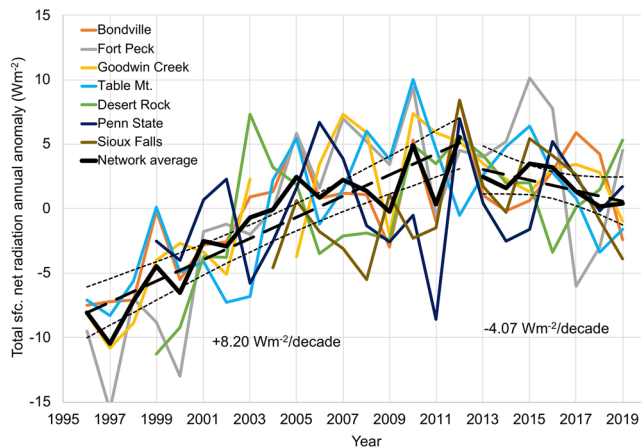
Figure 3. Same as Figure 2 but for total surface net radiation.

tempered behavior must be due to the response of surface net longwave to systematic changes of solar input, that is, brightening, and is scrutinized by examining surface net SW and net LW separately.

Figure 4 shows time series of surface net shortwave (SW↓ – SW↑), or SW_{net}, net longwave (LW↓ – LW↑), or LW_{net}, and cloud fraction annual anomalies. It is obvious that SW_{net} and LW_{net} are anticorrelated. This behavior is primarily a response to cloud activity, as demonstrated in Figure 4 by the anticorrelation of mean cloud fraction and SW_{net}, and the positive correspondence of cloud fraction to LW_{net}. Relatively high cloud fraction anomalies (more clouds) generally correspond to greater LW_{net} and less SW_{net}, and vice versa for low cloud fraction anomalies. Although, variability of snow cover, aerosols, water vapor, cloud properties, and air temperature could also modulate the degree of contrast between SW_{net} and LW_{net}. As brightening progresses, the combined tendencies of SW_{net} and LW_{net} temper the transition of Q* from increasing to decreasing well before the dramatic change of SW↓ in 2013. Regardless of the high variability shown in Figure 4, the increasing trend of SW_{net} during the

brightening period (6.7 ± 1.5 Wm^{-2}/decade) is statistically significant according to MK analysis and has a low uncertainty. With the caveat of high variability, LW_{net} increases from 1996 to 2003 and then appears to taper off from 2004 to 2012. The LW_{net} trend during the brightening period (1.3 ± 1.1 Wm^{-2}/decade), with its high uncertainty relative to the mean, is not statistically significant according to MK. However, the values of these trends are not particularly relevant; it is how SW_{net} and LW_{net} evolve over time that is revealing. The apparent slowing of the LW_{net} trend after 2003 is likely a response to increasing SW↓. As brightening progresses, LW_{net} decreases, or at least levels off, in response to fewer clouds. More solar at the surface leads to greater skin temperatures and an increase LW↑, while at the same time, less clouds act to decrease LW↓, causing LW_{net} to decrease. This slowing of the LW_{net} trend in the latter part of the brightening period likely causes Q* to show a less abrupt transition from increasing to decreasing. After 2012 surface SW_{net} is less than it would have been if brightening continued, and surface LW_{net} is generally greater than during the brightening period. These tendencies point to greater cloud cover from 2013 to 2019. Another point of
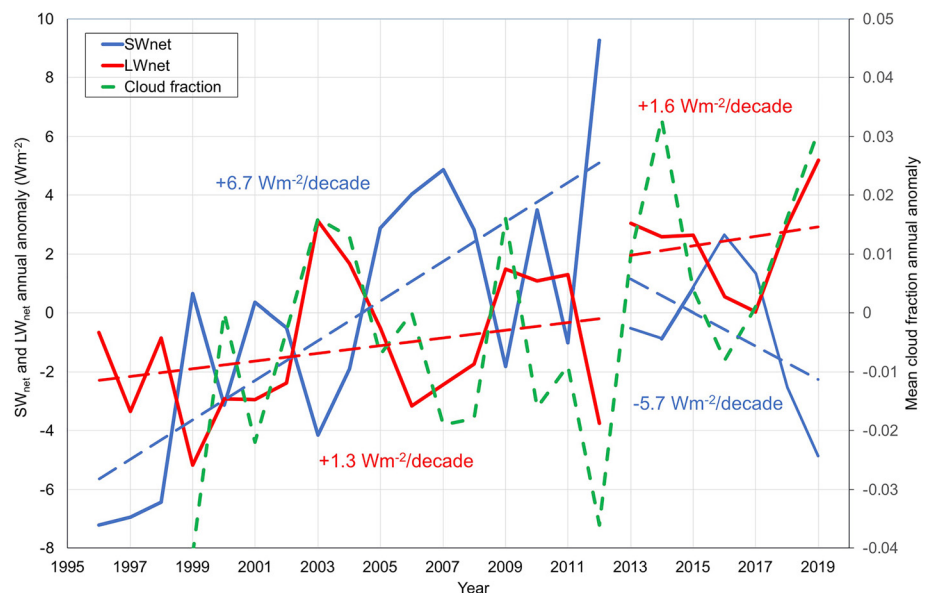

Figure 4. Time series of surface SW_{net} (blue) and surface LW_{net} (red) annual anomalies for the SURFRAD network (left *y*-axis). The horizontal zero line represents the long-term average over the length of each time series. Blue and red dashed lines are slopes of linear least-squares fits to the SW_{net} and LW_{net} time series, respectively, computed separately for 1996–2012 and 2013–2019. The green dashed curve represents network mean cloud fraction annual anomalies (right *y*-axis).
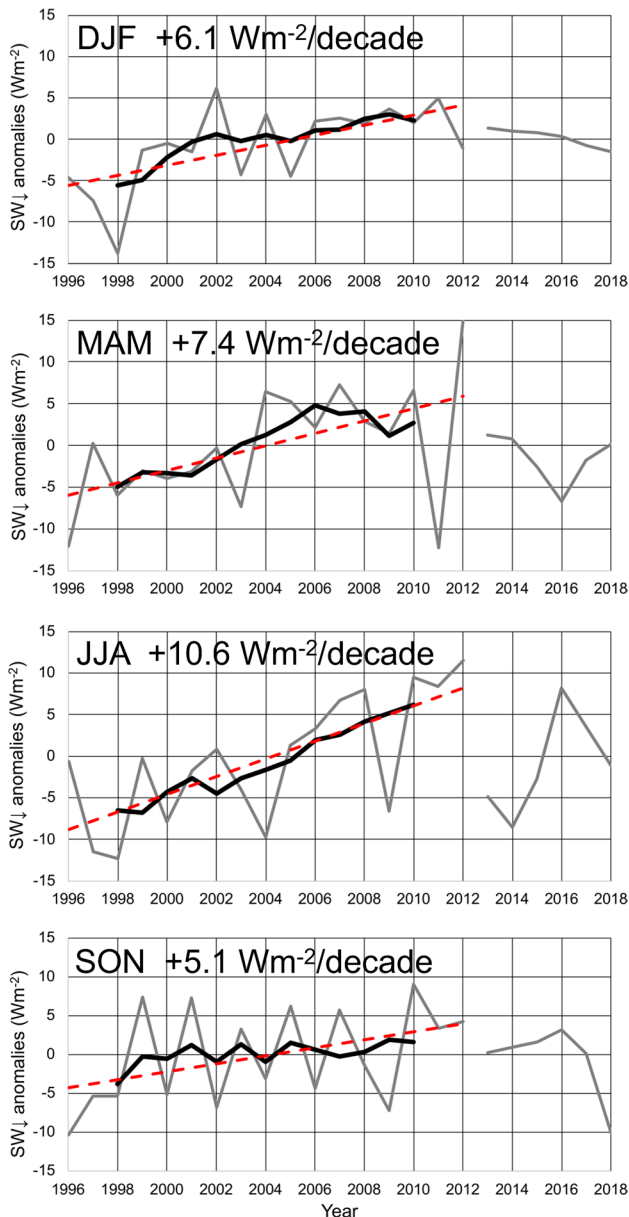
Figure 5. Time series of surface SW↓ seasonal anomalies. The horizontal zero lines represent the long-term average over the length of each time series. Seasons are defined as December-January-February (DJF), March-April-May (MAM), June-July-August (JJA), and September-October-November (SON). Gray curves are SW↓ seasonal anomalies, black curves are 5-year running means, and the red dashed lines are linear least-squares fits to the SW↓ seasonal anomalies of the brightening period (1996–2012). Brightening trends listed in each frame are the slopes of the linear least squares fits. Uncertainties associated with the trends shown are ±2.0 Wm^{-2} for DJF, ±3.1 Wm^{-2} for MAM, ±2.7 Wm^{-2} for JJA, and ±2.9 Wm^{-2} for SON.

interest is that after 2012 the decreasing trend of SW$_{net}$ is greater than that of SW↓ in Figure 2. This difference is likely due to the interannual variability of snow cover. For example, the average annual anomaly of upwelling solar for 2019 (not shown) is the second highest of the entire SURFRAD record and corresponds to the precipitous drop in SW$_{net}$ evident that year in Figure 4. Last, because SW$_{net}$ is a daytime quantity and LW$_{net}$ operates both day and night, LW$_{net}$ was examined for diurnal bias by computing daytime and nighttime trends separately. Results (not shown) demonstrate that LW$_{net}$ variability and trends are the same for day and night, revealing no diurnal bias. The primary difference is that nighttime LW$_{net}$ annual anomalies are about half the magnitude of those in the daytime.

4.2. Seasonal Trends of SW↓ at the Surface

Seasonal trends of SW↓ during the brightening period are shown in Figure 5, with associated uncertainties given in the figure caption. Comparing the mean seasonal trends with their uncertainties provides confidence that some degree of brightening occurred in all seasons. Furthermore, the transition from brightening to dimming is evident in all seasons. It is clear that because of greater insolation during the warmer seasons the absolute degree of brightening is greater in summer (JJA) and spring (MAM). Summer shows the greatest absolute increase of 17 Wm^{-2} over the brightening period, while the other seasons show smaller increases of 12 (MAM), 10 (DJF), and 8 (SON) Wm^{-2}. These differences are evident in the five-year running means shown in Figure 5 (dark curves). However, DJF shows the largest relative increase of SW↓ (10.5%), while the other seasons have smaller relative increases of ~6%. All but SON have statistically significant increasing trends during the brightening period according to MK analysis. Presumably, the trend for SON is not statistically significant because of high interannual variability. A seasonal analysis for Europe by Sanchez-Lorenzo et al. (2015) finds similar results, including the greatest absolute degree of brightening in summer. The period after 2012 was not analyzed seasonally because of the small sample size.

Long et al. (2009) and Augustine and Dutton (2013) attribute brightening over the U.S. from 1996 through the first decade of the 2000s to decreasing cloud cover and de-emphasize the role of aerosols. This updated analysis for the U.S. shows that clouds continue to be the primary influence on SW↓ at the surface. High interannual variability of cloud fraction annual anomalies shown in Figure 6 precludes the establishment of meaningful trends, but long-term-average comparisons are suggestive of a significant change after 2012. The network mean cloud fraction for the brightening period (horizontal red dashed line in Figure 6 from 1999 to 2012) is 2.4% less than the mean cloud fraction of the dimming period (2013–2019). The first three years are not used because only three stations had acceptable cloud fraction data during those years. That the standard error of the two long-term averages do not overlap suggests that the cloud populations of the two periods are statistically different.

A proven way to examine trends in cloudiness is through sun duration measurements. Chapter 8 of the WMO Guide to Instruments and Methods of Observation (World Meteorological Organization, 2008) states that sunshine duration measurements are equivalent to pyrheliometer (direct-normal) measurements that exceed 120 Wm^{-2}, and that sunshine duration measurements are inversely related to cloudiness. In clear conditions the 120 Wm^{-2} threshold is achieved within a half hour
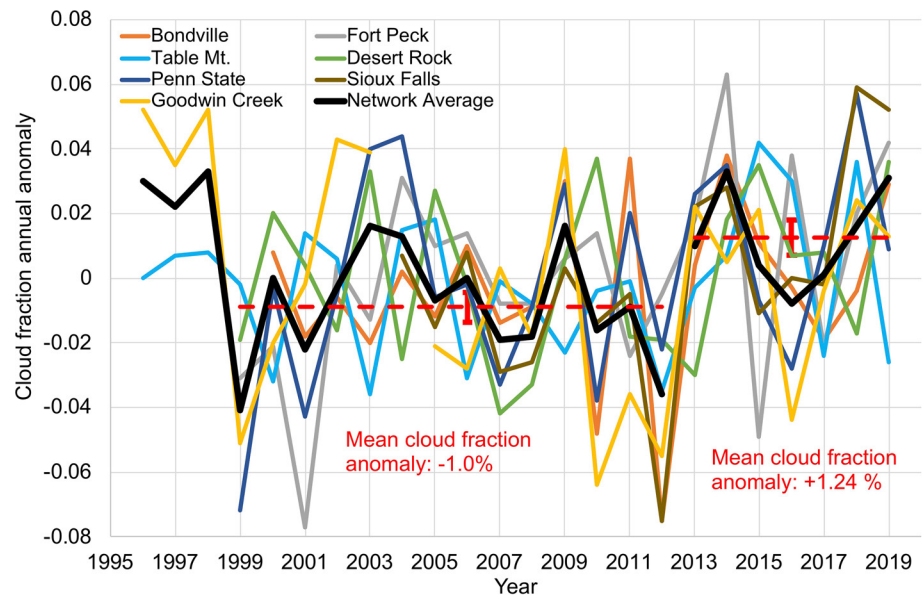
Figure 6. Time series of cloud fraction annual anomalies. The horizontal zero line represents the long-term average over the length of the time series. The thick black curve represents the network mean and color-coded curves are annual cloud fraction anomalies of individual stations. The two horizontal red dashed lines represent the mean cloud fraction anomaly for the brightening and dimming periods, and the vertical red bars represent the standard error of the annual anomalies of the two periods.

after sunrise and a half hour before sunset. Unlike the cloud fraction data, for which the first 3 years could not be used, SURFRAD direct-normal measurements were of sufficient quality that all years could be included in this analysis. Figure 7 shows that direct-normal SW annual anomalies increased by 11.7 ± 3.6 W/ m^{-2}/decade during the brightening period, but with only 41% of the variance explained. Three anomalous years in the 17-year brightening period (1999, 2001, 2009) were responsible for the low R^2 value. With those years removed, the trend increases to 16.5 ± 2.5 Wm^{-2}/decade, with 78% of the variance explained (not shown). Figure 7 also shows that direct-normal SW annual anomalies decreased after 2012. Given
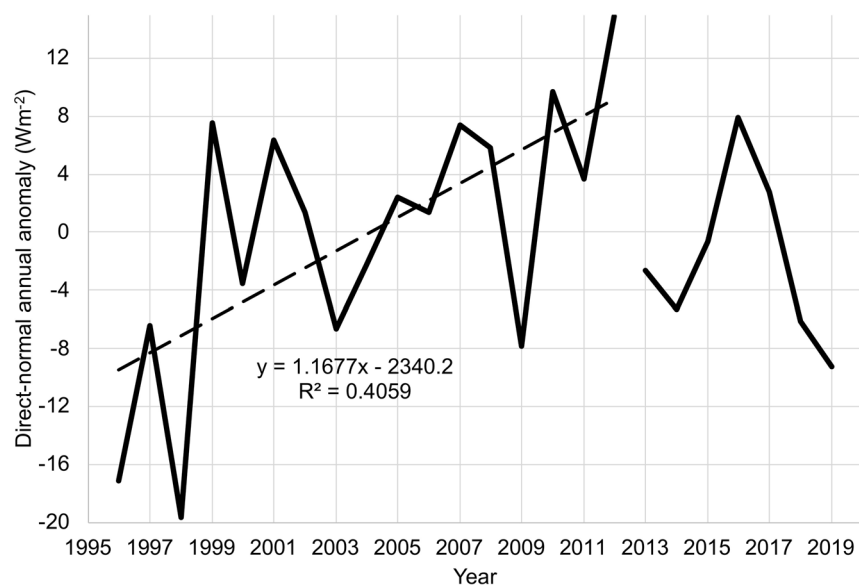

Figure 7. Time series of network annual average anomalies of direct-normal SW irradiance at the surface. The horizontal zero line represents the long-term average over the length of the time series. The dashed line is the linear least squares fit to the time series over the brightening period from 1996 to 2012.
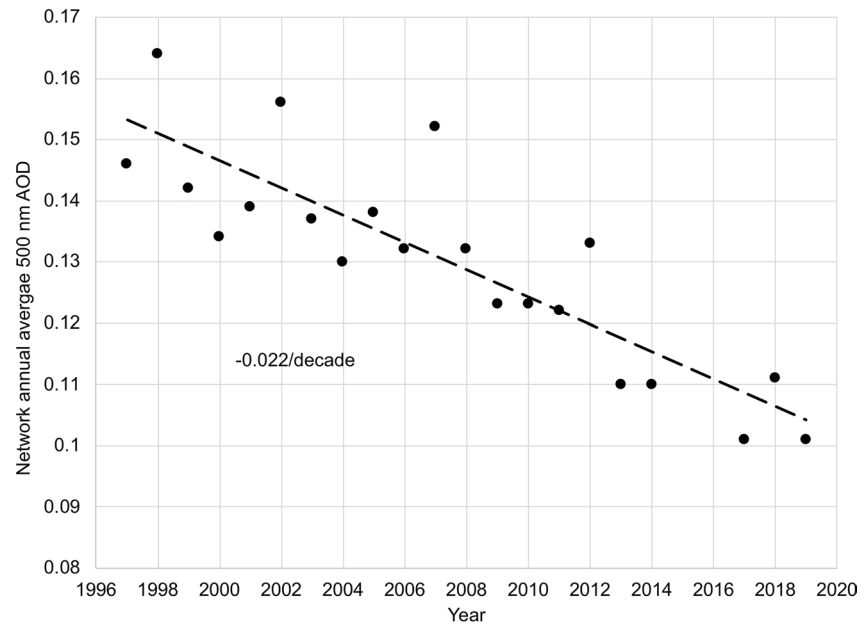
Figure 8. Time series of network annual average 500 nm aerosol optical depth (AOD). The dashed line is a linear least squares fit to the time series.

the inverse relationship between sunshine duration measurements and cloudiness, this analysis provides viable evidence that cloud cover systematically decreased over the U.S. during the brightening period and increased during the dimming period. Seasonally, trends in direct-normal irradiance are positive in all seasons with summer (JJA) showing the greatest increase of 17.4 ± 5.6 Wm^{-2}/decade and lowest uncertainty. The other seasons also have appreciable positive trends in direct-normal irradiance of 10.5 ± 7.8 (SON), 8.7 ± 6.5 (MAM), and 7.9 ± 6.6 (DJF) Wm^{-2}/decade, but with high uncertainties. These results indicate that the effect of clouds on brightening was consistently active in summer. Greater uncertainties in other seasons denotes a high interannual variability of cloud cover that would modulate the effects of clouds on surface solar radiation from year to year during those seasons.

Regarding aerosols, Figure 8 shows the network mean 500 nm AOD continuously decreasing by 0.022 ± 0.003 per decade over the tenure of the SURFRAD network. Decreasing AOD should act to increase SW↓ at the surface through both the direct (Mitchell, 1971) and second indirect effect (Albrecht, 1989) of aerosols, yet the period analyzed encompasses 17 years of brightening followed by seven years of dimming. Applying equation 2 of Augustine and Dutton (2013) reveals that the 0.05 reduction of AOD from 1997 to 2019 corresponds to a direct radiative forcing of $+1.59$ Wm^{-2}. The actual change in SW↓ during the brightening period from 1996 to 2012 is $+11.77$ Wm^{-2}, and that for the dimming period is -2.35 Wm^{-2}. Both of these period-wide changes are greater in magnitude than the computed direct effect of aerosols for the observed change in AOD. Further, the continued reduction of AOD beyond 2012 as SW↓ decreased is inconsistent with the computed direct forcing of aerosols and argues for a diminished role of the direct effect to the observed trends of SW↓. The second indirect effect of aerosols influences SW↓ by reducing (increasing) the extent of cloud cover and cloud lifetime with decreasing (increasing) aerosols. According to Ten Hoeve and Augustine (2016) the magnitude of decreasing AOD over the first 17 years of the SURFRAD network could account for a ~1% decrease in cloud fraction, which is seen in Figure 6, and plausibly contribute to the observed brightening. However, it is unlikely that the second indirect effect played any role in the dimming that followed because with AOD continuing to decrease after 2012, the mean cloud fraction should have *decreased* by 0.28% according to Ten Hoeve and Augustine (2016). Instead, it *increased* by over 2%. That behavior casts doubt on the role of the second indirect effect of aerosols on brightening or dimming in the U.S.

Last, AOD and cloud fraction annual anomalies are compared to network-wide SW↓ annual anomalies using linear regression. Figure 9a demonstrates that clouds account for 62% of the interannual variability

(a)
y = -0.0041x + 0.0004
R² = 0.6219

(b)
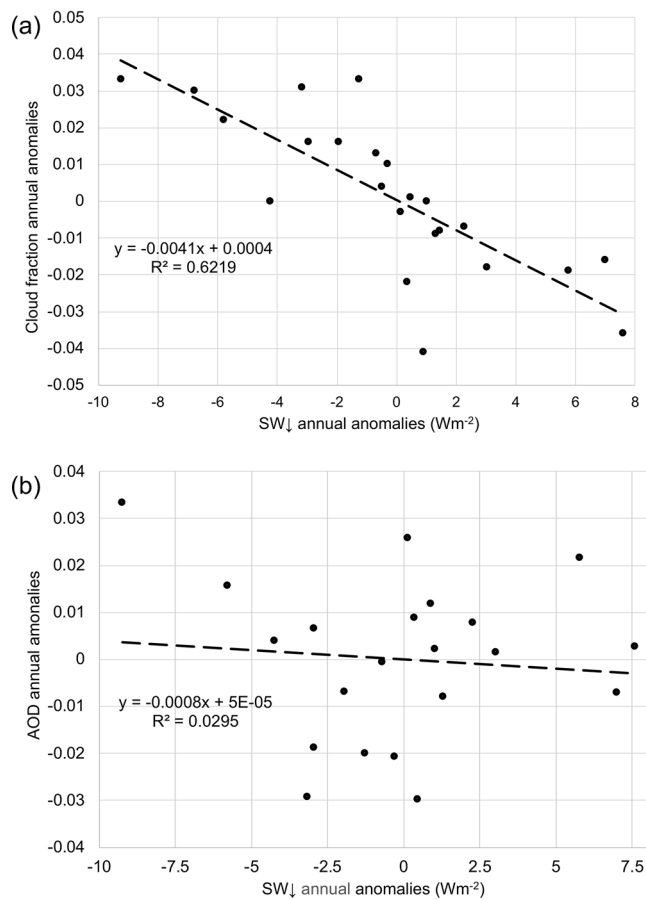y = -0.0008x + 5E-05
R² = 0.0295

Figure 9. (a) Network cloud fraction annual anomalies versus SW↓ annual anomalies with linear least squares fit (dashed line), linear fit equation, and R^2 value. (b) Same as (a) but for network AOD annual anomalies versus SW↓ annual anomalies.

of SW↓, and alternately, Figure 9b shows that AOD accounts for only 3% of SW↓ variability. While these analyses can't be used to attribute the observed SW↓ trends to clouds or aerosols, they do show that cloud variability is a dominant factor in the interannual variability of all-sky SW↓. This result, together with the evidence that sun duration increased through the brightening period and decreased in the dimming period directs follow on research to look at physical mechanisms that cause systematic decadal-scale changes in cloud cover.

5. Summary and Conclusions

Long-term variability of surface radiation budget components over the U.S. has been updated through 2019 using SURFRAD Network data. A primary result is that brightening in the U.S. appears to have ended in 2012. Significant brightening of solar irradiance at the surface of $+7.36 \pm 1.47$ Wm^{-2}/decade is documented from 1996 to 2012, however, based on other studies, U.S. brightening extends back to the mid-to-late 1980s. Brightening through 2012 is observed at all stations except Penn State, which shows no trend through 2012, indicating that the network average trend represents much of the contiguous 48 states with the possible exception of the Northeast. In 2013, downwelling shortwave at the surface abruptly decreased to the long-term mean and remained somewhat stable for 5 years through 2017. Decreases in the following two years resulted in a -3.90 ± 3.1 Wm^{-2}/decade dimming trend from 2013 to 2019. The brevity of this period along with the large uncertainty on the trend indicates that it is too early to place a definitive value on the new tendency of surface solar irradiance after 2012. We can only conclude that some degree of dimming or stabilization has commenced. Seasonally, the transition from brightening to diminished surface solar irradiance after 2012 is evident in all seasons. Absolute brightening is more robust in summer, but relative increases are largest in winter, albeit with greater uncertainty.

Observed trends of surface solar irradiance are more consistent with changes in cloud cover than aerosols. This association is especially evident in the time series of direct-normal solar annual anomalies, which are directly related to sun duration and inversely related to cloudiness. Network average direct-normal shortwave irradiance increases by 11.7 ± 3.6 Wm^{-2}/decade during the brightening period (16.5 ± 2.5 Wm^{-2}/decade when three anomalous years are excluded) and decreases after 2012. These trends indicate decreasing cloud cover during the brightening period and increasing cloud cover in the dimming period. Appreciable increases in direct-normal irradiance are also evident in all seasons during the brightening period, especially in summer. Other seasons show smaller increases of direct-normal irradiance with higher uncertainties. In support, the long-term average cloud fraction over the brightening period is 2.4% less than during the dimming period that follows.

AOD decreased by 0.022/decade from 1997 to 2019 over the U.S. The second indirect effect of aerosols, which relates aerosol amount to cloud area and lifetime, is consistent with this systematic decrease of AOD and less clouds during the brightening period, but at odds with the continuing decline of AOD and more clouds during the seven years of dimming that follows. A correlation analysis using all years of SURFRAD data show that cloud fraction annual anomalies explain 62% of the variance of surface solar irradiance, while annual anomalies of AOD account for only 3%. This dichotomy suggests clouds are mostly responsible for the variability of surface solar irradiance over the U.S., but statistically these correlations can't be linked to the observed trends. Total surface net radiation (Q*) shows the same general temporal behavior as surface solar irradiance but the change from an increasing to decreasing trend is more gradual. The slower variation of Q* is attributed to the response of surface net longwave to systematic changes in solar input

and its effect on clouds. The dominant influence of clouds on surface solar irradiance trends over the U.S. suggests a possible link to short-term climate variability, which also evolves in a decadal fashion.

Data Availability Statement

All SURFRAD Network data used are available from the Baseline Surface Radiation Network archive in Bremerhaven, Germany at https://dataportals.pangaea.de/bsrn/.

References

Albrecht, B. A. (1989). Aerosols, cloud microphysics, and fractional cloudiness. *Science*, *245*, 1227–1230. https://doi.org/10.1126/science.245.4923.1227

Alexander, M. A., Halimeda Kilbourne, K., & Nye, J. A. (2014). Climate variability during warm and cold phases of the Atlantic Multidecadal Oscillation (AMO) 1871-2008. *Journal of Marine Systems*, *133*, 14–26. https://doi.org/10.1016/j.jmarsys.2013.07.017

Augustine, J. A., Cornwall, C. R., Hodges, G. B., Long, C. N., Medina, C. I., & DeLuisi, J. J. (2003). An automated method of MFRSR calibration for aerosol optical depth analysis with application to an Asian dust outbreak over the United States. *Journal of Applied Meteorology and Climatology*, *42*, 266–278. https://doi.org/10.1175/1520-0450(2003)042<0266:aamomc>2.0.co;2. .

Augustine, J. A., DeLuisi, J. J., & Long, C. N. (2000). SURFRAD-A national surface radiation budget network for atmospheric research. *Bulletin of the American Meteorological Society*, *81*, 2341–2357. https://doi.org/10.1175/1520-0477(2000)081<2341:SANSRB>2.3.CO;2

Augustine, J. A., & Dutton, E. G. (2013). Variability of the surface radiation budget over the United States from 1996 through 2011 from high-quality measurements. *Journal of Geophysical Research - D: Atmospheres*, *118*, 43–53. https://doi.org/10.1029/2012JD018551

Augustine, J. A., Hodges, G. B., Cornwall, C. R., Michalsky, J. J., & Medina, C. I. (2005). An Update on SURFRAD-The GCOS Surface Radiation Budget Network for the Continental United States. *Journal of Atmospheric and Oceanic Technology*, *22*, 1460–1472. https://doi.org/10.1175/JTECH1806.1

Augustine, J., Dutton, E. G., Meyers, T., & Michalsky, J. (2006). *Scientific rationale for the placement of sites to monitor the surface energy budget for climate applications*. NOAA Tech. Memo, OAR GMD-17.

Bush, B. C., Valero, F. P. J., Simpson, A. S., & Bignone, L. (2000). Characterization of thermal effects in pyranometers: A data correction algorithm for improved measurement of surface insolation. *Journal of Atmospheric and Oceanic Technology.*, *17*, 165–175. https://doi.org/10.1175/1520-0426(2000)017<0165:coteip>2.0.co;2

Chylek, P., Dubey, M. K., Lesins, G., Li, J., & Hengartner, N. (2014). Imprint of the Atlantic multi-decadal oscillation and Pacific decadal Oscillation on southwestern US climate: Past, present, and future. *Climate Dynamics*, *43*, 119–129. https://doi.org/10.1007/s00382-013-1933-3

Dutton, E. G., Nelson, D. W., Stone, R. S., Longenecker, D., Carbaugh, G., Harris, J. M., & Wendell, J. (2006). Decadal variations in surface solar irradiance as observed in a globally remote network. *Journal of Geophysical Research*, *111*, D19101. https://doi.org/10.1029/2005JD006901

Enfield, D. B., Mestas-Nuñez, A. M., & Trimble, P. J. (20012077–2080). The Atlantic multidecadal oscillation and its relationship to rainfall and river flows in the continental US. *Geophysical Research Letters*, *28*. https://doi.org/10.1029/2000gl012745

Frohlich, C. (1991). History of solar radiometry and the World Radiometric Reference. *Metrologia*, *28*(3), 111–115. https://doi.org/10.1088/0026-1394/28/3/001

Gilgen, H., Wild, M., & Ohmura, A. (1998). Means and trends of shortwave irradiance at the surface estimated from global energy balance archive data. *Journal of Climate*, *11*, 2042–2061. https://doi.org/10.1175/1520-0442-11.8.2042

Gueymard, C. A., & Myers, D. R. (2008). Solar Radiation Measurement: Progress in Radiometry for Improved Modeling. In V. Badescu, (Ed.), *Modeling solar radiation at the earth's surface*. Berlin, Heidelberg: Springer. https://doi.org/10.1007/978-3-540-77455-6_1

Harrison, L., Michalsky, J., & Berndt, J. (1994). Automated multifilter rotating shadow-band radiometer: an instrument for optical depth and radiation measurements. *Applied Optics*, *33*, 5118–5125. https://doi.org/10.1364/ao.33.005118

Hatzianastassiou, N., Ioannidis, E., Korras-Carraca, M.-B., Gavrouzou, M., Papadimas, C. D., Matsoukas, C., et al. (2020). Global dimming and brightening features during the first decade of the 21st Century. *Atmosphere*, *11*(3), 308. https://doi.org/10.3390/atmos11030308

Hatzianastassiou, N., Matsoukas, C., Fotiadi, A., Pavlakis, K. G., Drakakis, E., Hatzidimitriou, D., & Vardavas, I. (2005). Global distribution of Earth's surface shortwave radiation budget. *Atmospheric Chemistry and Physics*, *5*, 2847–2867. https://doi.org/10.5194/acp-5-2847-2005

Herman, J., DeLand, M. T., Huang, L.-K., Labow, G., Larko, D., Lloyd, S. A., et al. (2013). A net decrease in the Earth's cloud, aerosol, and surface 340 nm reflectivity during the past 33 yr (1979-2011). *Atmospheric Chemistry and Physics*, *13*, 1–20. https://doi.org/10.5194/acp-13-1-201310.5194/acp-13-8505-2013

He, Y., Wang, K., Zhou, C., & Wild, M. (2018). A Revisit of Global Dimming and Brightening Based on the Sunshine Duration. *Geophysical Research Letters*, *45*, 4281–4289. https://doi.org/10.1029/2018GL07742410.1029/2018gl077424

Kendall, M. G. (1975). *Rank correlation methods*. London: Charles Griffin. ISBN: 0852641990 9780852641996.

Liepert, B. G. (2002). Observed reductions of surface solar radiation at sites in the United States and worldwide from 1961 to 1990. *Geophysical Research Letters*, *29*(10), 61. https://doi.org/10.1029/2002GL014910

Liepert, B. G., Fabian, P., & Grassl, H. (1994). Solar radiation in Germany: Observed trends and assessment of their causes: Part I. Regional approach. *Contributions to Atmospheric Physics*, *67*(1), 15–29.

Long, C. N., & Ackerman, T. P. (2000). Identification of clear skies from broadband pyranometer measurements and calculation of downwelling shortwave cloud effects. *Journal of Geophysical Research*, *105*, 15609–15626. https://doi.org/10.1029/2000JD900077

Long, C. N., Ackerman, T. P., Gaustad, K. L., & Cole, J. N. S. (2006). Estimation of fractional sky cover from broadband shortwave radiometer measurements. *Journal of Geophysical Research*, *111*, D11204. https://doi.org/10.1029/2005JD006475

Long, C. N., Dutton, E. G., Augustine, J. A., Wiscombe, W., Wild, M., McFarlane, S. A., & Flynn, C. J. (2009). Significant decadal brightening of downwelling shortwave in the continental United States. *Journal of Geophysical Research*, *114*, D00D06. https://doi.org/10.1029/2008JD011263

Mann, H. B. (1945). Nonparametric tests against trend. *Econometrica*, *13*, 245–259. https://doi.org/10.2307/1907187

McArthur, L. J. B. (2005). Baseline Surface Radiation Network (BSRN) Operations Manual. WMO/TD-No. 1274, WCRP/WMO.

McCabe, G. J., Palecki, M. A., & Betancourt, J. L. (2004). Pacific and Atlantic Ocean influences on multidecadal drought frequency in the United States. *Proceedings of the National Academy of Sciences*, *101*, 4136–4141. https://doi.org/10.1073/pnas.0306738101

Michalsky, J., Dutton, E. G., Nelson, D., Wendell, J., Wilcox, S., Andreas, A., et al. (2011). An extensive comparison of commercial pyrheliometers under a wide range of routine observing conditions. *Journal of Atmospheric and Oceanic Technology*, *28*, 752–766. https://doi.org/10.1175/2010JTECHA1518.1

Mitchell, J. M. (1971). The Effect of Atmospheric Aerosols on Climate with Special Reference to Temperature near the Earth's Surface. *Journal of Applied Meteorology and Climatology*, *10*, 703–714. https://doi.org/10.1175/1520-0450(1971)010<0703:TEOAAO>2.0.CO;2

Müller, B., Wild, M., Driesse, A., & Behrens, K. (2014). Rethinking solar resource assessments in the context of global dimming and brightening. *Solar Energy*, *99*, 272–282. https://doi.org/10.1016/j.solener.2013.11.013

Myers, D. R., Stoffel, T. L., Reda, I., Wilcox, S. M., & Andreas, A. M. (2002). Recent progress in reducing the uncertainty in and improving pyranometer calibrations. *Journal of Solar Energy Engineering*, *124*(1), 44–50. https://doi.org/10.1115/1.1434262

Nigam, S., Guan, B., & Ruiz-Barradas, A. (2011). Key role of the Atlantic Multidecadal Oscillation in 20th century drought and wet periods over the Great Plains. *Geophysical Research Letters*, *38*, L16713. https://doi.org/10.1029/2011gl048650

Ohmura, A. (2009). Observed decadal variations in surface solar radiation and their causes. *Journal of Geophysical Research*, *114*, D00D05. https://doi.org/10.1029/2008JD011290

Ohmura, A., Gilgen, H., Hegner, H., Müller, G., Wild, M., Dutton, E. G., et al. (1998). Baseline surface radiation network (BSRN/WCRP): New precision radiometry for climate research. *Bulletin of the American Meteorological Society*, *79*, 2115–2136. https://doi.org/10.1175/1520-0477(1998)079<2115:bsrnbw>2.0.co;2

Ohmura, A., & Lang, H. (1989). Secular variation of global radiation in Europe. In J. Lenoble & J.-F. Geleyn (Eds.), *IRS'88: Current Problems in Atmospheric Radiation* (pp. 298–301). Hampton: A. Deepak Publishing.

Philipona, R., Dutton, E. G., Stoffel, T., Michalsky, J., Reda, I., Stifter, A., et al. (2001). Atmospheric longwave irradiance uncertainty: Pyrgeometers compared to an absolute sky-scanning radiometer, atmospheric emitted radiance interferometer, and radiative transfer model calculations. *Journal of Geophysical Research*, *106*(D22), 28129–28141. https://doi.org/10.1029/2000jd000196. .

Sanchez-Lorenzo, A., Wild, M., Brunetti, M., Guijarro, J. A., Hakuba, M. Z., Calbó, J., et al. (2015). Reassessment and update of long-term trends in downward surface shortwave radiation over Europe (1939–2012). *Journal of Geophysical Research - D: Atmospheres*, *120*, 9555–9569. https://doi.org/10.1002/2015JD023321

Schwarz, M., Folini, D., Hakuba, M. Z., & Wild, M. (2017). Spatial representativeness of surface-measured variations of downward solar radiation. *Journal of Geophysical Research - D: Atmospheres*, *122*, 13319–13337. https://doi.org/10.1002/2017jd027261

Shaw, G. E. (1983). Sun photometry. *Bulletin of the American Meteorological Society*, *64*, 4–10. https://doi.org/10.1175/1520-0477(1983)064<0004:sp>2.0.co;2

Stanhill, G. (2005). Global dimming: A new aspect of climate change. *Wea*, *60*(1), 11–14. https://doi.org/10.1256/wea210.0310.1256/wea.210.03

Stanhill, G., & Moreshet, S. (1992). Global radiation climate changes: The world network. *Climatic Change*, *21*, 57–75. https://doi.org/10.1007/BF00143253

Sutton, R. T., & Dong, B. (2012). Atlantic Ocean influence on a shift in European climate in the 1990s. *Nature Geoscience*, *5*, 788–792. https://doi.org/10.1038/ngeo1595 https://doi.org/10.1038/ngeo1595

Ten Hoeve, J. E., & Augustine, J. A. (2016). Aerosol effects on cloud cover as evidenced by ground-based and space-based observations at five rural sites in the United States. *Geophysical Research Letters*, *43*, 793–801. https://doi.org/10.1002/2015GL066873

Thomas, A., Sarangi, C., & Kanawade, V. P. (2019). Recent Increase in Winter Hazy Days over Central India and the Arabian Sea. *Scientific Reports*, *9*, 17406. https://doi.org/10.1038/s41598-019-53630-3

Ting, M., & Wang, H. (1997). Summertime U.S. Precipitation variability and its relation to pacific sea surface temperature. *Journal of Climate*, *10*, 1853–1873. https://doi.org/10.1175/1520-0442(1997)010<1853:suspva>2.0.co;2

Tollenaar, M., Fridgen, J., Tyagi, P., Stackhouse Jr, P. W., & Kumudini, S. (2017). The contribution of solar brightening to the US maize yield trend. *Nature Climate Change*, *7*, 275–278. https://doi.org/10.1038/nclimate3234

Wang, K. (2014). Measurement biases explain discrepancies between the observed and simulated decadal variability of surface incident solar radiation. *Scientific Reports*, *4*(2014), 6144. https://doi.org/10.1038/srep06144

Wang, S., Huang, J., He, Y., & Guan, Y. (20142014). Combined effects of the Pacific Decadal Oscillation and El Niño-Southern Oscillation on Global Land Dry-Wet Changes Oscillation and El Ninõ-Southern Oscillation on Global Land Dry–Wet Changes. *Scientific Reports*, *4*, 6651. https://doi.org/10.1038/srep06651

Wild, M. (2009). Global dimming and brightening: A review. *Journal of Geophysical Research*, *114*, D00D16. https://doi.org/10.1029/2008JD011470

Wild, M. (2012). Enlightening global dimming and brightening.*Bulletin of the American Meteorological Society*, *93*, 27–37. https://doi.org/10.1175/BAMS-D-11-00074.1

Wild, M. (2016). Decadal changes in radiative fluxes at land and ocean surfaces and their relevance for global warming. *Bulletin of the American Meteorological Society*, *7*, 91–107. https://doi.org/10.1002/wcc.372

Wild, M., Gilgen, H., Roesch, A., Sanchez-Lorenzo, A., Long, C. N., Dutton, E. G., et al. (2005). Evidence for clear-sky dimming and brightening in central Europe. *Science*, *48*, 847–850. https://doi.org/10.1126/science.1103215

Wild, M., Trussel, B., Ohmura, A., Long, C. N., Konig-Langlo, G., Dutton, E. G., & Tsvetkov, A. (2009). From dimming to brightening: decadal changes in solar radiation at earth's surface. *Journal of Geophysical Research*, *114*, D00D13. https://doi.org/10.1029/2008JD011382

Wild, M., Wacker, S., Yang, S., & Sanchez-Lorenzo, A. (2021). Evidence for clear-sky dimming and brightening in central Europe. *Geophysical Research Letters*, *48*, e2020GL092216. https://doi.org/10.1029/2020GL092216

Willson, R. C., & Mordvinov, A. V. (2003). Secular total solar irradiance trend during solar cycles 21–23. *Geophysical Research Letters*, *30*, 1199. https://doi.org/10.1029/2002GL016038

World Meteorological Organization. (2008). *Guide to Instruments and Methods of Observation Volume 1 – Measurement of Meteorological Variables*. WMO-No. 8, Geneva, Switzerland. ISBN 978-92-63-10008-5.